Polymer 50 (2009) 4781–4787

Contents lists available at ScienceDirect

Polymer

journal homepage: www.elsevier.com/locate/polymer

Electrospinning zwitterion-containing nanoscale acrylic fibers

Rebecca H. Brown [a], Matthew T. Hunley [b], Michael H. Allen, Jr. [a], Timothy E. Long [a,*]

[a] Department of Chemistry, Macromolecules and Interfaces Institute, Virginia Tech, Blacksburg, VA 24061-0212, USA
[b] Macromolecular Science and Engineering Program, Virginia Tech, Blacksburg, VA 24061-0212, USA

ARTICLE INFO

Article history:
Received 21 May 2009
Received in revised form
8 August 2009
Accepted 10 August 2009
Available online 14 August 2009

Keywords:
Electrospinning
Ionomer
Zwitterion

ABSTRACT

Free radical copolymerization of *n*-butyl acrylate and a sulfobetaine methacrylamide derivative provided high molecular weight zwitterionic copolymers containing 6–13 mol% betaine functionality, and the electrospinning of low T_g zwitterionomers was explored for the first time. Copolymerizations were performed in dimethylsulfoxide (DMSO) rather than fluorinated solvents previously reported in the literature. Dynamic mechanical analysis of zwitterionomer films revealed biphasic morphology and featured a rubbery plateau and two distinct thermal transitions. Electrospinning from chloroform/ethanol (80/20 v/v) solutions at low concentrations between 2 and 7 wt% afforded nanoscale polymeric fibers with diameters near 100 nm. The presence of only 6 mol% zwitterion allowed the formation of low T_g, free-standing, non-woven mats, and we hypothesize that zwitterionic aggregation rather than chain entanglements facilitated electrospinning at these relatively low solution concentrations. To our knowledge, this is the first report of electrospun zwitterionic polymers and these non-woven membranes are expected to lead to new applications for sulfobetaine copolymers.

1. Introduction

The electrospinning process employs an electrostatic potential to form micro- and nanoscale fibers, resulting in thin fibrous mats with high surface area and submicron pores [1–4]. Electrospinning occurs when a charged polymer solution or melt emits a jet in the presence of an electric field [5]. The jet travels rapidly in a chaotic, whip-like motion to a grounded target where solid fibers collect in the form of three-dimensional, non-woven mats [6]. Several important factors, including solution conductivity, viscosity, applied voltage, and tip-to-target distance, dictate the size and morphology of collected fibers [7,8]. Solution concentration has the largest effect on fiber diameter, where higher polymer concentrations lead to the formation of thicker fibers. Applications of electrospun fibers include filtration devices, membranes, protective clothing, tissue scaffolds, and nanofiber-based sensors and electrodes [9–14].

Previous reports demonstrated that successful electrospinning requires the presence of chain entanglements within the polymer solution [15,16]. The electrospinning behavior of neutral polyesters as a function of molecular weight and solution concentration was previously studied in our laboratories [15]. The critical concentration for entanglements (C_e) was the minimum concentration needed for fiber formation, while defect-free fibers required concentrations above $2C_e$. Later, Wnek and coworkers [16] developed a semi-empirical model for predicting the limits of fiber formation for a range of polymers in good solvents without the presence of polymer–polymer interactions. Fiber formation was correctly predicted to occur in the presence of more than 2.5 entanglements per polymer chain, while one entanglement per chain led to beaded morphologies. While sufficient chain entanglements encourage fiber formation, entanglements are not a required condition to form uniform fibers. Rutledge et al. [17] evaluated the role of fluid elasticity, independent of other fluid properties, in electrospinning a series of non-entangled aqueous solutions of poly(ethylene glycol) containing small amounts of high molecular weight poly(ethylene oxide). Bead-on-string and uniform fibers were collected for the elastic solutions electrospun at low concentrations and low shear viscosities ($<$0.30 Pa s), and bead formation did not occur under any condition. The researchers concluded that fluid elasticity sufficiently stabilized the polymer jet on the short time scale of electrospinning, leading to uniform fiber formation in the absence of chain entanglements.

For ion-containing polymers, the presence of intramolecular electrostatic interactions significantly affects the solution conformation, leading to differences in entanglement behavior. Long et al. [3] studied the electrospinning of poly(2-(dimethylamino)ethyl methacrylate hydrochloride) in water/methanol, and found that concentrations of $8C_e$ were required to form defect-free fibers. The charges in the polyelectrolyte side chains created

* Corresponding author. Tel.: +1 540 231 2480; fax: +1 540 231 8517.
E-mail address: telong@vt.edu (T.E. Long).

0032-3861/$ – see front matter © 2009 Elsevier Ltd. All rights reserved.
doi:10.1016/j.polymer.2009.08.017

instabilities in the electrospinning jet that required much higher viscosities to suppress. The high electrical conductivity of the polyelectrolyte solutions led to fibers 2–3 orders of magnitude smaller than neutral polymers electrospun from solutions of similar viscosity and concentration. The addition of NaCl to polyelectrolyte solutions resulted in the screening of electrostatic interactions and a decrease in the normalized concentration required for fiber formation. Ionic aggregation also drastically alters solution conformation and polymer chain dynamics. Elabd et al. [18] explored the electrospinning behavior of Nafion® under various conditions, and discovered that pure Nafion® solutions were highly aggregated and lacked sufficient entanglements to stabilize the electrospinning jet. Blending Nafion® with poly (acrylic acid) suppressed ionic aggregation, and nanoscale Nafion® fibers were collected. Understanding the interplay of viscosity, concentration, and aggregation in electrospun charged polymers remains a fundamental interest.

Polybetaines are a class of zwitterionic polymers featuring a covalently bound cation and anion on each repeating unit. Sulfobetaines feature a quaternized ammonium and a sulfonate group tethered through an alkylene spacer. Polybetaines mimic lipid structures found in biological membranes, which has led to numerous biological applications, including anti-biofouling and protein resistant coatings, biomedical devices, and antimicrobial surfaces [19–21]. Incorporation of sulfobetaine monomers into various polymer matrices offers many potential advantages, including water dispersibility or solubility and mechanical toughness resulting from ionic aggregation.

Galin et al. [22] copolymerized sulfobetaine-based monomers with *n*-butyl acrylate (*n*BA) and 2-ethoxyethyl acrylate (EEA). When placed in a nonpolar matrix with a low T_g, the polar zwitterions aggregated to form strong physical crosslinks similar to classic ionomers. Thermal and mechanical analysis revealed a biphasic morphology consisting of the nonpolar matrix and an ion-rich phase. Later, Gauthier et al. also copolymerized a series of different sulfobetaine monomers with *n*BA and EEA to explore the effects of zwitterionic structure on aggregation behavior [23]. Dynamic mechanical analyses revealed an increased rubbery modulus at higher sulfobetaine concentrations, which was consistent with an increased degree of ionic crosslinking.

To our knowledge, electrospinning of betaine-containing copolymers is unprecedented. In this work, we synthesized a series of *n*-butyl acrylate-based low T_g copolymers containing low concentrations of a zwitterionic monomer (6–13 mol%). We report the effects of zwitterion concentration on the mechanical properties and electrospinning behavior of the copolymers. Incorporation of zwitterionic functionalities offers a method to electrospin nanoscale fibers from very low solution concentrations. Zwitterion-containing fibers enable potential applications in membrane technologies, antimicrobial surfaces, and protective clothing.

2. Experimental section

2.1. Materials

N-(3-sulfopropyl)-*N*-methacryloylamidopropyl-*N*,*N*-dimethylammonium betaine (SBMAm) was provided by Raschig GmbH (Germany) and used without purification. Dimethylsulfoxide (DMSO, 99.9+%), azobisisobutyronitrile (AIBN), and *n*-butyl acrylate (*n*BA) were purchased from Sigma-Aldrich Chemical Co. AIBN was recrystallized from methanol. *n*BA was passed through a neutral alumina column to remove inhibitors and then distilled under reduced pressure from CaH_2. Chloroform, ethanol, and ethyl acetate were purchased from VWR and used without further purification.

2.2. Synthesis of poly(n-butyl acrylate-co-sulfobetaine methacrylamide) (PnBA-co-PSBMAm)

A typical copolymerization is described. *n*BA (5.0 g, 0.039 mol) and SBMAm (1.27 g, 0.004 mol) were added to a 100 mL, round-bottomed flask with a magnetic stir bar. The reaction mixture was diluted with DMSO (51 mL, 90 wt%), and AIBN (31.4 mg, 0.50 wt%) was added to the reaction vessel. The reaction mixture was sparged with nitrogen for 15 min and placed in an oil bath at 60 °C for 24 h. The polymer was precipitated into approximately 4 L of water and dried under reduced pressure. Residual DMSO was further removed using either Soxhlet extraction in ethyl acetate or vacuum distillation at 60 °C. The isolated polymer was dried under reduced pressure at 80 °C for 48 h and stored in a desiccator. Isolated yields after precipitation and extraction were typically 75%.

2.3. Synthesis of poly(n-butyl acrylate) (PnBA)

*n*BA (25 g, 0.195 mol), AIBN (170 mg, 0.001 mol), and ethyl acetate (110 mL, 80 vol%) were added to a 250 mL, round-bottomed flask equipped with a magnetic stir bar. The reaction was sparged with nitrogen for 15 min and placed in an oil bath at 65 °C for 22 h. The reaction solution was diluted with 150 mL ethyl acetate, and added drop wise to 5 L of 9:1 methanol/water solution. The isolated polymer was dried at reduced pressure at 60 °C for 18 h to yield 22.6 g (90% yield).

2.4. Electrospinning

Zwitterionic copolymers were dissolved in 80/20 v/v chloroform/ethanol at 7 wt%. Subsequent concentrations were achieved through a series of dilutions. P*n*BA was dissolved in 80/20 v/v chloroform/ethanol at concentrations of 5 and 30 wt%. The polymer compositions and concentration ranges analyzed are summarized in Table 1. The solutions were placed in a 20-mL syringe that was mounted in a syringe pump (KD Scientific Inc). The positive lead of a high voltage power supply (Spellman CZE1000R, Spellman High Voltage Electronics Corp.) was connected to an 18-gauge syringe needle using an alligator clip. A grounded metal target (304 stainless steel mesh screen) was placed 20 cm from the needle tip. The syringe pump delivered the polymer solution at a controlled flow of 3 mL/h, and the voltage was maintained at 25 kV. Constant electrospinning conditions were maintained in order to isolate the effect of zwitterion content on the fiber morphology and diameter. Electrospun mats were stored in a desiccator until SEM images were obtained.

2.5. Instrumentation

^{1}H NMR spectra of the polymers were obtained on a Varian Unity 400 spectrometer in $CDCl_3$ at 399.95 MHz. Molar compositions were determined using resonance integrals at 0.94 ppm for the $-CH_3$ of *n*BA and the $-CH_3$ groups on the quaternary ammonium of SBMAm at 3.33 ppm, according to previous methods [23]. Size exclusion chromatography (SEC) was used to determine the molecular weights of zwitterionomers at 50 °C in *N*,*N*-dimethyformamide

Table 1
Summary of polymers and concentration ranges for electrospinning study.

Polymer composition	Concentration range (wt%)
P*n*BA$_{94}$-*co*-PSBMAm$_6$	2.0–6.7
P*n*BA$_{90}$-*co*-PSBMAm$_{10}$	1.5–7
P*n*BA$_{87}$-*co*-PSBMAm$_{13}$	2.0–6.8
P*n*BA	5, 30

(DMF) with 0.01 M lithium bromide (LiBr) at 1 mL min^{-1}. DMF SEC was performed on a Waters SEC equipped with two Waters Styragel HR5E (DMF) columns, a Waters 717plus autosampler, and a Waters 2414 differential refractive index detector. Reported molecular weights are relative to polystyrene standards. SEC of P*n*BA was performed in tetrahydrofuran at 40 °C and 1 mL min^{-1} on a Waters SEC equipped with three Polymer Laboratories PLGel 5 μm Mixed-C columns. THF SEC instrumentation included a Waters 717plus autosampler, Waters 2414 differential refractive index detector, and a Wyatt Technologies miniDAWN multiangle laser light scattering (MALLS) detector. Absolute molecular weight is reported, using a d*n*/dc of 0.07.

Dynamic mechanical analysis (DMA) was conducted on a TA Instruments Q800 dynamic mechanical analyzer in tension mode at a frequency of 1 Hz and a temperature ramp of 3 °C/min. All films were solution cast from chloroform on Teflon® molds and dried for 72 h at 70 °C at reduced pressure (0.4 mm Hg) prior to analysis. Steady shear rheological experiments were performed with a TA Instruments AR-G2 rheometer at 25 °C using concentric cylinder geometry. Copolymer solutions in chloroform/ethanol (80/20 v/v) were analyzed using shear rate sweeps from 0.01 to 1000 s^{-1}. The lower torque limit was set at 0.01 μN m, and the error of the measurement was determined to be ±2%.

Electrospun fiber diameter and morphology were analyzed using a Leo 1550 field emission scanning electron microscope (FESEM). Fibers for FESEM analysis were collected on a ¼ in × ¼ in stainless steel mesh, mounted on a SEM disk, and sputter-coated with an 8 nm Pt/Au layer to reduce electron charging effects. Twenty measurements on random fibers for each electrospinning condition were performed using the provided SEM software package to determine average fiber diameters and standard deviations. Error bars shown represent one standard deviation.

3. Results and discussion

3.1. Synthesis of zwitterionic copolymers

Copolymers consisting of *n*BA and SBMAm were synthesized via AIBN-initiated free radical copolymerization (Scheme 1). Identification of a suitable solvent to afford homogeneous reactions posed a synthetic challenge due to the drastic polarity differences between the two monomers. Ehrmann and Galin reported using ethanol as the reaction solvent for the copolymerization of SBMAm and *n*BA; however, reactions became heterogeneous for $f_{SBMAm} < 0.1$ [22]. Gauthier and coworkers used 2,2,2-trifluoroethanol for the copolymerization of *n*BA and a sulfobetaine methacrylate derivative with feed compositions of 1–70 mol% zwitterion, while maintaining homogeneous solutions only to 30% monomer conversion [24]. Other solvents with their monomer system, including DMSO, tetrahydrofuran, and DMF, resulted in heterogeneous reactions as both zwitterion and total monomer concentrations increased [24]. In this work, polymerizations in DMSO afforded homogeneous reactions to complete conversion with zwitterion monomer feed compositions up to 13 mol% and total monomer concentration maintained at 10 wt%. This strategy offers a viable alternative to more expensive fluorinated solvents commonly used in the literature.

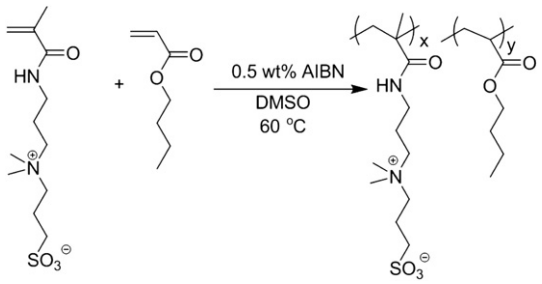

Scheme 1. Synthesis of poly(*n*-butyl acrylate-*co*-sulfobetaine methacrylamide) (P*n*BA-*co*-PSBMAm).

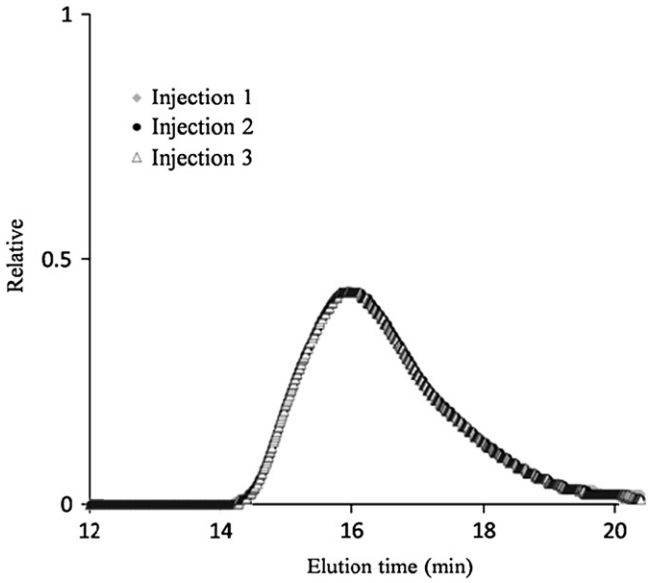

Fig. 1. Reproducible SEC chromatograms of P*n*BA$_{90}$-*co*-PSBMAm$_{10}$.

Isolated zwitterionic copolymers were insoluble in most organic solvents except chloroform, hot DMSO, and DMF. Chloroform was utilized in this study for film casting and electrospinning. Copolymer compositions were determined with ^{1}H NMR spectroscopy in $CDCl_3$, and results agreed well with the monomer feed ratios (±1 mol%). Zwitterion contents of 6, 10, and 13 mol% were achieved. The zwitterionic content was designed to systematically explore the effects of sulfobetaine on the mechanical properties and electrospinning behavior. In addition, molecular weight characterization was achieved using SEC in DMF with 0.01 M LiBr, where the salt content effectively inhibited aggregation and screened polymer–column interactions for reproducible results. Representative chromatograms exhibiting reproducibility of three consecutive injections are shown in Fig. 1 for P*n*BA$_{90}$-*co*-PSBMAm$_{10}$. Copolymer molecular weights relative to polystyrene standards are shown in Table 2.

3.2. Dynamic mechanical analysis of zwitterionic copolymers

Ionomers are known to form biphasic morphologies exhibiting two glass transition temperatures. These distinct thermal transitions represent ion-rich and ion-poor regions formed through the aggregation of ionic groups. DMA measurements of zwitterionic copolymer films were performed in order to monitor the effect of zwitterion concentration on the thermal transitions and mechanical

Table 2
Relative molecular weights of zwitterionic copolymers.

Copolymer	M_w (g/mol)	M_w/M_n
P*n*BA$_{94}$-*co*-PSBMAm$_6$	519,000	2.42
P*n*BA$_{90}$-*co*-PSBMAm$_{10}$	344,000	2.65
P*n*BA$_{87}$-*co*-PSBMAm$_{13}$	259,000	2.75

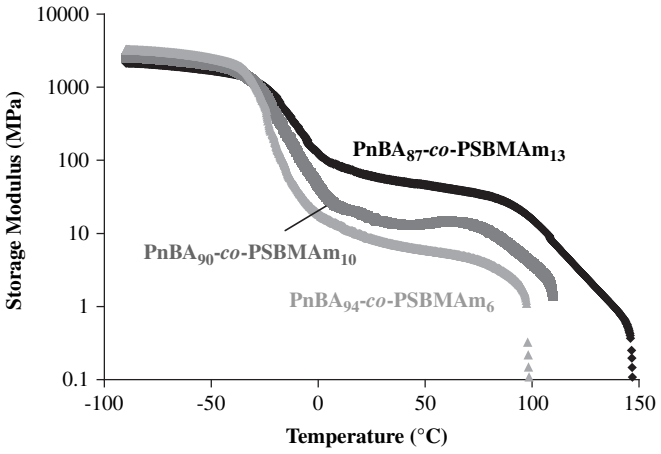

Fig. 2. Storage modulus at 1 Hz as a function of temperature for P*n*BA-*co*-PSBMAm containing 6, 10, and 13 mol% SBMAm.

properties. Copolymer films were dried at reduced pressure for 72 h at 70 °C prior to analysis in order to minimize the effects of water absorption.

The storage moduli as a function of temperature for a series of P*n*BA-*co*-PSBMAm compositions are shown in Fig. 2. An increase in both the T_g of the ion-poor matrix phase and the breadth of the transition was observed as the SBMAm content increased from 6 to 13 mol%. This trend was also observed in previous studies of SBMAm copolymers with poly(*n*BA) [25] and poly(EEA) [26], as well as *n*BA-based copolymers with sulfobetaine methacrylate derivatives [24]. All of the zwitterionomers also exhibited a rubbery plateau region, which was attributed to thermally labile physical crosslinks formed within the ionic aggregates [24]. The modulus of the rubbery plateau region increased with zwitterion content, representing an increased number of crosslink sites. A second thermal transition, attributed to the T_g of the ion-rich phase, occurred at approximately 80 °C for all three copolymers. DMA of P*n*BA-*co*-PSBMAm films with only 6 mol% zwitterion content is in sharp contrast to low T_g P*n*BA, which is a viscous liquid at room temperature that does not form films and could not be analyzed using DMA. Previous reports of the thermal properties of P*n*BA using a dynamic mechanical thermal analyzer showed only one transition at the T_g of P*n*BA with flow at 0 °C, and no presence of a rubbery plateau region [25]. This major difference in mechanical properties demonstrated the electrostatic interaction between zwitterionic groups, which allowed the formation of free-standing films.

3.3. Electrospinning nanoscale fibers

Electrospinning studies of P*n*BA-*co*-PSBMAm at three zwitterion contents were performed at constant conditions (25 kV, 3 mL/h, 20 cm tip-to-target distance) in order to isolate the effects of concentration on fiber formation. To our knowledge, electrospinning of zwitterion-containing copolymers was not reported earlier. The copolymers were electrospun from 80/20 v/v chloroform/ethanol solutions at concentrations below 7 wt%. Ethanol was added as a cosolvent for electrospinning to decrease solvent volatility and prevent clogging of the syringe tip.

3.3.1. Effect of solution concentration on fiber morphology

Many studies have demonstrated the effect of solution concentration on fiber diameter and morphology during the electrospinning process. Fig. 3 shows the effect of solution concentration on the fiber morphology of P*n*BA$_{90}$-*co*-PSBMAm$_{10}$ electrospun fibers. At the lowest concentration of 1.5 wt%, polymer beads or droplets were observed with very few fibers present. Polymer droplets form when insufficient elasticity is present to withstand the Raleigh instabilities and stabilize the charged electrospun jet [2]. The phenomenon of droplet formation is known as electrospraying.

Electrospinning of P*n*BA$_{90}$-*co*-PSBMAm$_{10}$ occurred at solution concentrations greater than 1.5 wt% to form nanometer- to micron-sized fibers. Beaded fiber morphologies formed between 2 and 3 wt%, while uniform bead-free fibers formed above 4 wt%. Similar trends in fiber morphology were observed for P*n*BA$_{94}$-*co*-PSBMAm$_6$ and P*n*BA$_{87}$-*co*-PSBMAm$_{13}$, as shown for selected concentrations in Fig. 4. The minimum concentration required for uniform electrospun fibers was correlated to C_e for linear and branched neutral polyesters in our laboratories [27], and for poly(vinyl alcohol) by Shivkumar et al. [28]. In the case of neutral polymers, uniform

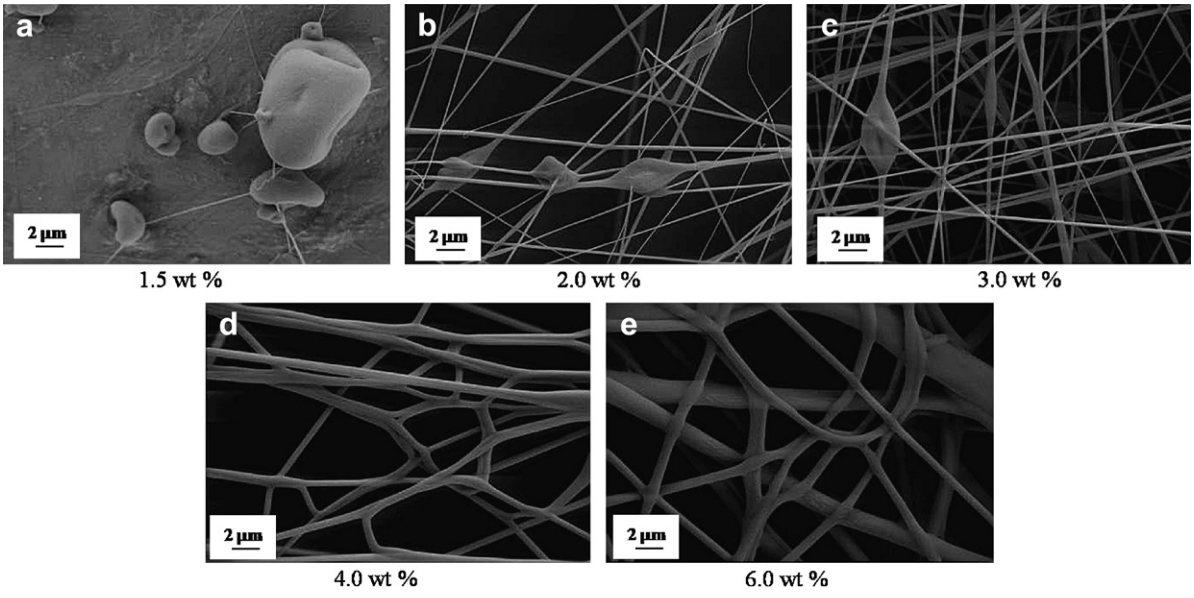

Fig. 3. FESEM images of P*n*BA$_{90}$-*co*-PSBMAm$_{10}$ electrospun fibers at various solution concentrations in chloroform/ethanol (80/20 v/v).

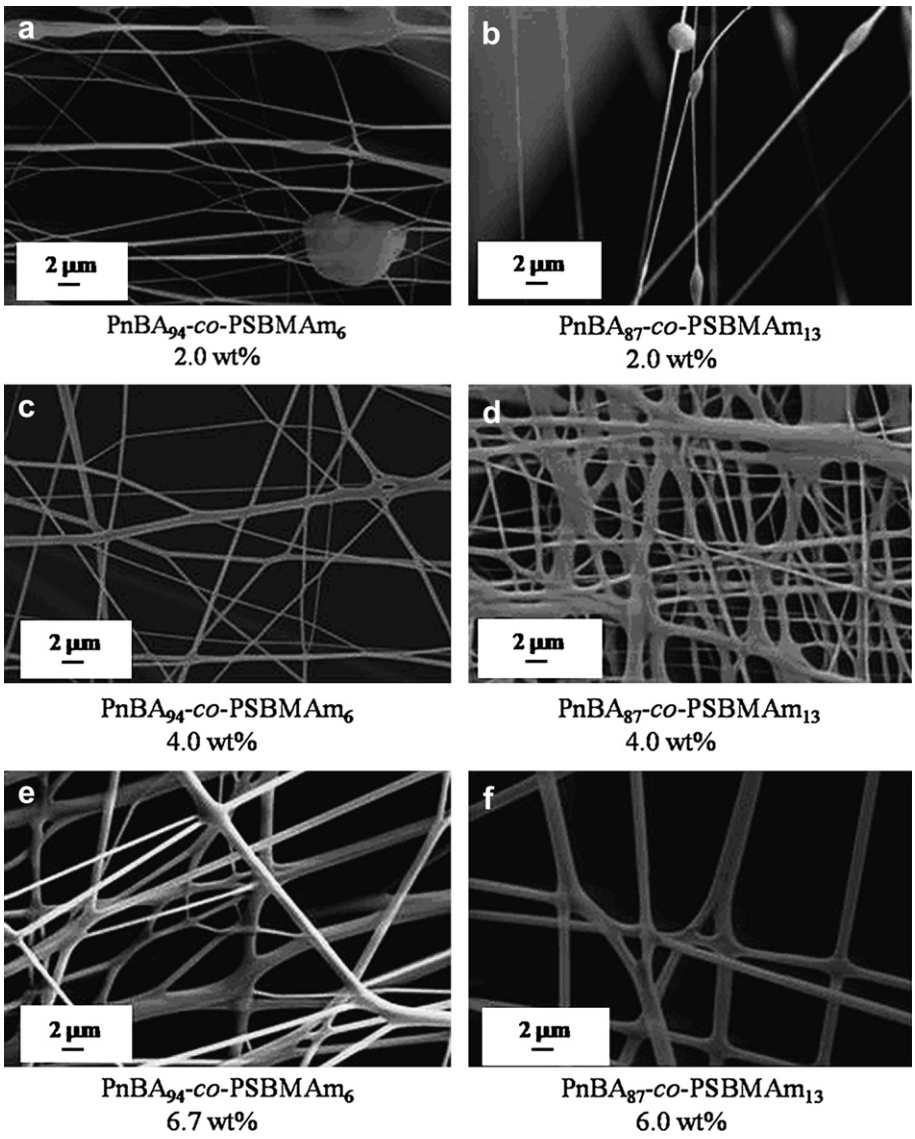

Fig. 4. FESEM images of electrospun fibers of P*n*BA$_{94}$-*co*-PSBMAm$_6$ and P*n*BA$_{87}$-*co*-PSBMAm$_{13}$ at increasing solution concentrations in chloroform/ethanol (80/20 v/v).

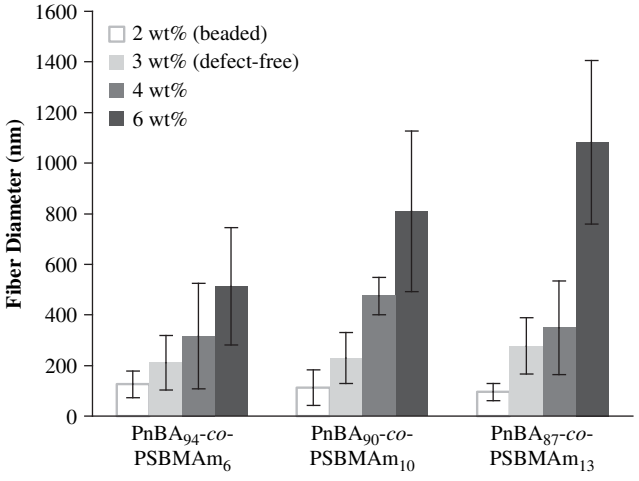

Fig. 5. Average fiber diameters of P*n*BA$_{94}$-*co*-PSBMAm$_6$, P*n*BA$_{90}$-*co*-PSBMAm$_{10}$, and P*n*BA$_{87}$-*co*-PSBMAm$_{13}$ as a function of solution concentration in chloroform/ethanol (80/20 v/v).

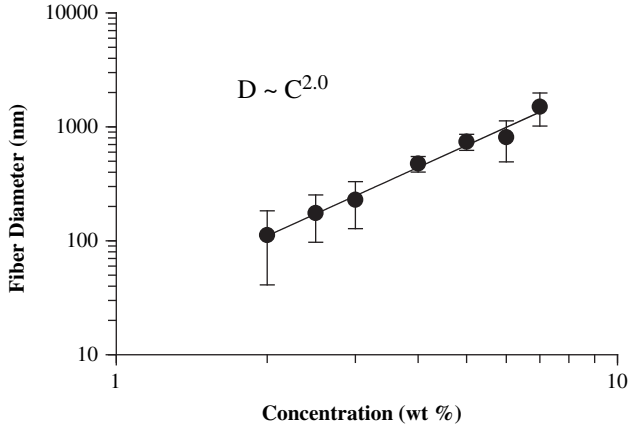

Fig. 6. Dependence of fiber diameter on solution concentration for P*n*BA$_{90}$-*co*-PSBMAm$_{10}$.

Table 3
Fiber diameter scaling exponents for copolymers of various zwitterion concentrations.

Copolymer	Power law dependence	Avg. fiber diameter at 3.0 wt%
P*n*BA$_{94}$-*co*-PSBMAm$_6$	1.3	211 ± 108
P*n*BA$_{90}$-*co*-PSBMAm$_{10}$	2.0	229 ± 101
P*n*BA$_{87}$-*co*-PSBMAm$_{13}$	2.3	277 ± 111

fibers were commonly observed at concentrations above $2C_e$. For zwitterionomers, the onset of fiber formation occurred at 2 wt% regardless of zwitterion content, and bead-free fibers were collected at 4 wt% for all compositions.

The fusion of electrospun thin fibers was observed periodically throughout the study for each of the copolymer compositions. This phenomenon was most prominent in the thicker fibrous mats where fibers were collected on the target for longer times. Fiber fusion likely occurred due to a combination of insufficient solvent evaporation during the jet lifetime and the low T_g matrix of *n*BA-based copolymers. Areas where distinct fibers fused together after collection are clearly visible in Fig. 4d.

3.3.2. Effect of solution concentration on fiber diameter

Continuous fibers approximately 1–2 μm in diameter were collected after electrospinning from 7 wt% solutions. Fiber diameters systematically decreased with solution concentration, reaching average diameters of approximately 100 nm at the lowest concentration for fiber formation (2 wt%). Fig. 5 shows the fiber diameter as a function of solution concentration for all three copolymer compositions. Fiber diameters are reported as the average of 20 measurements from different areas of the fibrous mat, and the error bars represent one standard deviation of this average. The chaotic nature of the electrospinning process typically causes variations in fiber diameter of approximately 30%. Larger standard deviations were measured for P*n*BA-*co*-PSBMAm, partially due to the presence of fused fibers.

The concentration dependence of P*n*BA$_{90}$-*co*-PSBMAm$_{10}$ electrospun fiber diameter is shown in Fig. 6. The fiber diameter exhibited a 2.0 power law dependence on concentration. A slight variation in power law dependence was observed with changing SBMAm content. The fiber diameter scaling exponents as a function of zwitterion content are tabulated in Table 3. Despite a much larger M_w of P*n*BA$_{94}$-*co*-PSBMAm$_6$ compared to P*n*BA$_{90}$-*co*-PSBMAm$_{10}$ and P*n*BA$_{87}$-*co*-PSBMAm$_{13}$, the power law dependence increased with zwitterion content. While equivalent molecular weights at each zwitterion concentration are required to isolate the effect of charge, this trend indicated that ionic interactions were the primary dominant factors during electrospinning.

3.3.3. Influence of zwitterion aggregation on the electrospinning process compared to neutral P*n*BA

The ability to form mechanically robust non-woven fibrous mats from low T_g copolymers containing low zwitterion loadings is a significant result that demonstrates the strong interaction between zwitterion functionalities. For comparison, electrospinning of high molecular weight (M_w 283,000 g/mol) P*n*BA was attempted at two different solution concentrations as shown in Fig. 7. At 5 wt% (Fig. 7a), a concentration analogous to the electrospinning conditions for zwitterionic copolymers, fibers did not form and polymer droplets were collected on the grid. Electrospinning was also performed at a much higher concentration of 30 wt%, which corresponds to a concentration of approximately $2C_e$ (where C_e was measured as 15 wt% in chloroform for P*n*BA of M_w 278,000 g/mol using previously reported rheological techniques [15]). At 30 wt%, a large continuous fiber jet was visible during the electrospinning process as expected based on previous results for neutral polymers. However, fibers were not observed in the FESEM because the low T_g polymer flowed onto the collection grid prior to microscopy characterization. A P*n*BA fiber can be seen after flowing to cover one strand of the stainless steel mesh in Fig. 7b. This result shows that the incorporation of only 6 mol% zwitterionic functionality in a low T_g polymer matrix enabled the formation of stable, free-standing non-woven mats at room temperature without the need for post-processing conditions (ex. UV crosslinking) to maintain fiber structure.

In addition to drastic differences in concentration required for successful electrospinning between neutral P*n*BA and zwitterionomers, large differences in solution viscosities were also observed. The dependence of viscosity on shear rate for zwitterionic copolymers and P*n*BA is shown in Fig. 8. Flow curves for the zwitterionic copolymers exhibited Newtonian behavior, while P*n*BA appeared to exhibit shear thinning behavior at higher concentrations. The concentrations shown represent values above the onset of defect-free fiber formation (5 wt%) for P*n*BA-*co*-PSBMAm, and the rheologically predicted onset for P*n*BA (30 wt%). The viscosity of P*n*BA was two orders of magnitude greater than the P*n*BA-*co*-PSBMAm series, consistent with the entanglements present in a high concentration polymer solution. Zero-shear viscosities of the P*n*BA-*co*-PSBMAm series were between 0.022 and 0.032 Pa s. As expected based on molecular weight, P*n*BA$_{94}$-*co*-PSBMAm$_6$ (M_w 519,000 g/mol) exhibited the highest viscosity of the series. Viscosities of P*n*BA$_{90}$-*co*-PSBMAm$_{10}$ (M_w 344,000 g/mol) and P*n*BA$_{87}$-*co*-PSBMAm$_{13}$ (M_w 259,000 g/mol) were similar, but also scaled with molecular weight.

The drastic difference in solution concentrations and solution viscosities required for successful electrospinning of P*n*BA-*co*-PSBMAm and P*n*BA demonstrated a fundamental difference in the electrospinning process for these polymers. Acrylic polymers such

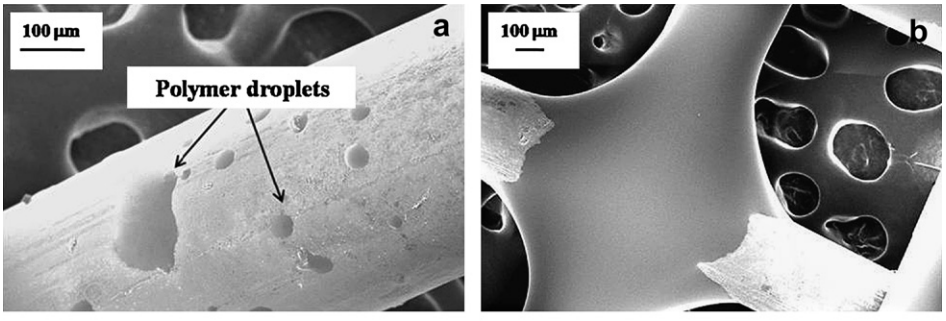

Fig. 7. FESEM images of low T_g P*n*BA (M_w 278,000 g/mol, $M_w/M_n = 2.56$) after attempted electrospinning from chloroform/ethanol (80/20 v/v) at different solution concentrations: (a) at 5.0 wt%, electrospraying of droplets onto collection grids occurred; (b) at 30 wt%, fibers were initially collected but flowed onto grid prior to analysis.

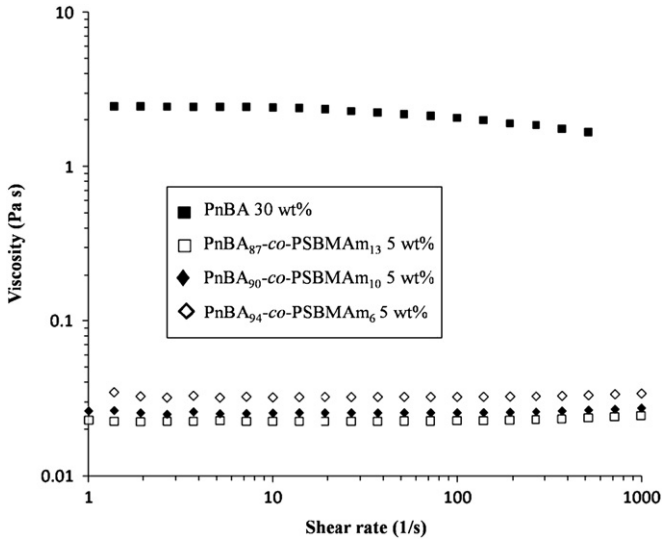

Fig. 8. Dependence of viscosity on shear rate for zwitterionomers and P*n*BA at concentrations (in 80/20 v/v chloroform/ethanol) equivalent to defect-free fiber formation.

as P*n*BA typically have large entanglement molecular weights (M_e), meaning high solution concentrations are required for entanglements and successful electrospinning (such as 30 wt% required to electrospin high molecular weight P*n*BA). However, continuous fibers were electrospun from P*n*BA-*co*-PSBMAm at 5 wt%, an order of magnitude lower than the concentration required for P*n*BA. In addition, the zero-shear viscosities of zwitterionomers at 4 wt% were two orders of magnitude lower than P*n*BA at $2C_e$. Solution viscosities of approximately 0.02 Pa s for zwitterionomers are the lowest viscosities observed for successful electrospinning in our laboratories [15], and are an order of magnitude lower than the low viscosity PEG/PEO solutions reported by Rutledge [17]. These results suggested that ionic associations rather than chain entanglements likely dominated the electrospinning process for zwitterionic copolymers at relatively low concentrations. Rheological studies of the zwitterionomer solutions are underway to confirm this hypothesis.

4. Conclusions

Zwitterionic copolymers featuring 6–13 mol% sulfobetaine in a P*n*BA matrix were electrospun from 80/20 v/v chloroform/ethanol solutions containing 2–7 wt% polymer to form robust nanoscale fibers. The presence of electrostatic interactions between zwitterionic groups in the soft P*n*BA matrix enabled the formation of free-standing fibers and films at room temperature. To our knowledge, this is the first report of electrospun zwitterionic copolymers. A transition from beaded morphology to uniform continuous fibers occurred at polymer concentrations of 4 wt% for each copolymer composition. Zwitterion incorporation enabled formation of fibers at low solution concentrations and viscosities below 0.02 Pa s, resulting in average fiber diameters as small as 100 nm. These viscosity values are the lowest observed for successful electrospinning in our laboratories, and are an order of magnitude lower than the PEG/PEO elastic solutions reported by Rutledge and coworkers [17]. Solution concentrations and viscosities required for the successful electrospinning of zwitterionic copolymers were orders of magnitude lower than required for high molecular weight PnBA. We hypothesize that intermolecular interactions rather than chain entanglements dominate the electrospinning process in copolymers featuring zwitterion aggregation. This method offers a new approach for the processing of nanoscale fibers at low concentrations with the introduction of a low concentration of strongly dipolar groups. These zwitterionic copolymers may be useful as stimuli responsive materials, electroactive devices, and elastomers, and the formation of non-woven membranes is expected to lead to additional new applications for zwitterionic copolymers.

Acknowledgements

This material is based upon work supported by the U.S. Army Research Laboratory and the U.S. Army Research Office under grant number W911NF-07-1-0339.

References

[1] Doshi J, Reneker DH. J Electrost 1995;35:151–60.
[2] Fong H, Chun I, Reneker DH. Polymer 1999;40:4585–92.
[3] McKee MG, Hunley MT, Layman JM, Long TE. Macromolecules 2006;39:575–83.
[4] McKee MG, Layman JM, Cashion MP, Long TE. Science 2006;311:353–5.
[5] Reneker DH, Chun I. Nanotechnology 1996;7:216–23.
[6] Shin YM, Hohman MM, Brenner MP, Rutledge GC. Polymer 2001;42:9955–67.
[7] Gupta P, Elkins CL, Long TE, Wilkes GL. Polymer 2005;46:4799–810.
[8] Greiner A, Wendorff JH. Angew Chem Int Ed 2007;46:5670–703.
[9] Kenawy E-R, Layman JM, Watkins JR, Bowlin GL, Matthews JA, Simpson DG, et al. Biomaterials 2003;24:907–13.
[10] Grafe T, Graham K. Int Nonwovens J 2003;12:51–5.
[11] Matthews JA, Wnek GE, Simpson DG, Bowlin GL. Biomacromolecules 2002;3:232–8.
[12] Wang XY, Drew C, Lee SH, Senecal KJ, Kumar J, Sarnuelson LA. Nano Lett 2002;2:1273–5.
[13] Hunley MT, Long TE. Polym Int 2008;57:385–9.
[14] Gibson P, Schreuder-Gibson H, Rivin D. Colloids Surf A 2001;187-188:469–81.
[15] McKee MG, Wilkes GL, Colby RH, Long TE. Macromolecules 2004;37:1760–7.
[16] Shenoy SL, Bates WD, Frisch HL, Wnek GE. Polymer 2005;46:3372–84.
[17] Yu JH, Fridrikh SV, Rutledge GC. Polymer 2006;47:4789–97.
[18] Chen H, Snyder JD, Elabd YA. Macromolecules 2008;41:128–35.
[19] Ward M, Sanchez M, Elasri MO, Lowe AB. J Appl Polym Sci 2006;101:1036–41.
[20] Kudaibergenov S, Jaeger W, Laschewsky A. Adv Polym Sci 2006;201:157–224.
[21] Lowe AB, McCormick CL. Chem Rev 2002;102:4177–89.
[22] Ehrmann M, Galin JC. Polymer 1992;33:859–65.
[23] Gauthier M, Carrozzella T, Penlidis A. J Polym Sci Part A Polym Chem 2002;40:511–23.
[24] Gauthier M, Carrozzella T, Snell G. J Polym Sci Part B Polym Phys 2002;40:2303–12.
[25] Ehrmann M, Muller R, Galin JC, Bazuin CG. Macromolecules 1993;26:4910–8.
[26] Bazuin CG, Zheng YL, Muller R, Galin JC. Polymer 1989;30:654–61.
[27] McKee MG, Park T, Unal S, Yilgor I, Long TE. Polymer 2005;46:2011–5.
[28] Koski A, Yim K, Shivkumar S. Mater Lett 2003;58:493–7.